COMPEL: The International Journal for Computation and Ma... in Electrical and Electronic Engineering

Convergence behaviour of coupled pressure and thermal networks

Andreas Blaszczyk Reto Flückiger Thomas Müller Carl-Olof Olsson

Convergence behaviour of coupled pressure and thermal networks

Andreas Blaszczyk and Reto Flückiger
ABB Corporate Research, Baden-Dättwil, Switzerland
Thomas Müller
Fakultät für Informatik, I10 (LRR), Technische Universität München, Garching, Germany, and
Carl-Olof Olsson
ABB Corporate Research, Västeras, Sweden

Abstract

Purpose – The purpose of this paper is to present a method for thermal computations of power devices based on a coupling between thermal and pressure networks. The concept of the coupling as well as the solution procedure is explained. The included examples demonstrate that the new method can be efficiently used for design of transformers and other power devices.

Design/methodology/approach – The bidirectional propagation of temperature signal is introduced to the pressure network, which enables control of the power flow and a close coupling to the thermal network. The solution method is based on automatic splitting of the network definition (netlist) into two separate networks and iteratively solving the model using the Newton-Raphson approach as well as the adaptive relaxation enhanced by the direction change control.

Findings – The proposed approach offers reliable convergence behaviour even for models with unknown direction of the fluid flow (bidirectional flows). The accuracy is sufficient for engineering applications and comparable with the computational fluid dynamics method. The computation times in the range of milliseconds and seconds are attractive for using the method in engineering design tools.

Originality/value – The new method can be considered as a foundation for a consistent network modelling system of arbitrary thermodynamic problems including fluid flow. Such a modelling system can be used directly by device designers since the complexity of thermodynamic formulations is encapsulated in predefined network elements while the numerical solution is based on a standard network description and solvers (Spice).

Keywords Transformers, Heat transfer, Power devices, Network analysis (circuits), Thermal modelling
Paper type Research paper

1. Introduction

The network approach has been traditionally used for thermal simulations of electric power devices (Gramsch *et al.*, 2007; Loebl, 1984). It is considered as a compromise between simple engineering calculations based on thermodynamic formulas and the computational fluid dynamics (CFD) that requires detailed discretization of the whole model volume. The fundamental advantage of the network approach is its ability to handle complex heat transfer models including conduction, radiation and convection. Thanks to an acceptable accuracy and the moderate computational effort it is traditionally used by designers of power devices for the analysis of temperature rise tests for arrangements like transformers with their cooling systems as well as switchgear components and subsystems. The main drawback of the traditional thermal network is related to a proper representation of mass flow phenomena that are typically handled in a rather rudimental way. This issue is addressed in this paper.

COMPEL: The International Journal for Computation and Mathematics in Electrical and Electronic Engineering
Vol. 33 No. 4, 2014
pp. 1233-1250

0332-1649
DOI 10.1108/COMPEL-12-2012-0378

We present a concept of coupling the thermal network with a new representation of a pressure network that is extended by a temperature propagation feature. The first attempts to solve such a coupled network have shown that the convergence behaviour is a limiting issue (Gramsch *et al.*, 2007). A new solution method that enables reliable computations of the coupled network as well as its convergence behaviour are presented in this paper. We illustrate our concepts and results using power transformer examples. However, the proposed method is generic and can be applied to any heat transfer problem involving fluid flow.

2. Network concept

Let us consider a power transformer represented as a simple thermal model (see Figure 1). It consists of a coil submerged in a fluid as a heating device and a radiator as a cooling device dissipating heat to the ambient air. The circulation of the fluid through the coil and the radiator keeps the temperature of the coil within the required limit. The flow of the fluid determines the topology of the extended pressure network shown in Figure 2(a). Each "fluid flow wire" (red, thick line in the middle) is assisted by two "temperature wires" (thin, green lines) that enable propagation of the fluid temperature along the network according to the computed direction of the flow (upwards or downwards). The coupling to the thermal network is realized by the "Branch" element. This element creates a temperature jump $\Delta\vartheta$ between its inlet and outlet according to the following equation:

$$P = |\dot{m}| c_p \Delta\vartheta \tag{1}$$

where P is the power flowing from/to the thermal network via a "fluid node" (denoted in Figure 2 as "FN1", "FN2", etc.), $|\dot{m}|$ the magnitude of mass flow rate through the "fluid flow wire", c_p the specific heat of the fluid. The temperature changes along the "Branch" are propagated always in the direction of the fluid flow. But, this direction is *a priori* not known and must be obtained as a solution of the pure pressure network. Therefore, two wires of the temperature network are required to enable propagation of the temperature signal in both directions.

In addition to "Branch" the changes of fluid temperatures are controlled by "Node" elements. A "Node" enables mixing of fluid streams at different temperatures. Both elements "Branch" and "Node" provide a consistent mechanism of controlling

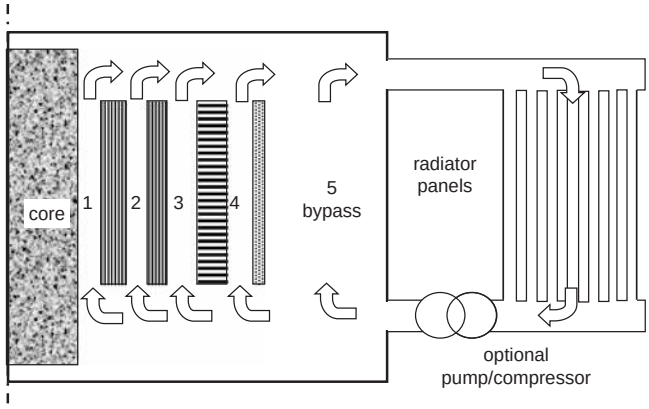

Figure 1.
Transformer coil and radiator as a thermal model with fluid circulation

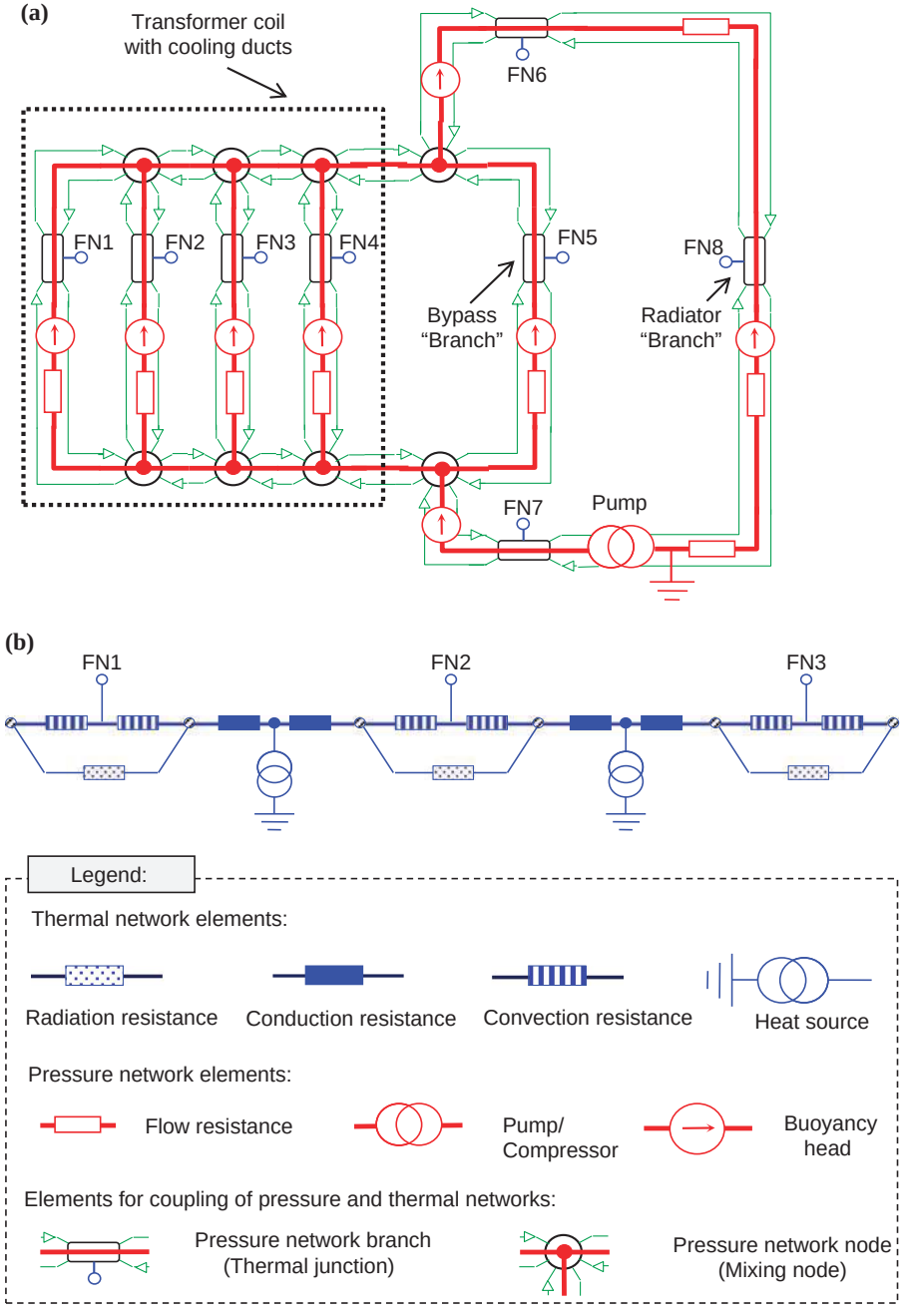

Figure 2.
(a) Extended pressure network for the transformer model in Figure 1; (b) part of the thermal network (for two inner winding segments of the coil and adjacent ducts)

temperature across the pressure network. In this way, the extended pressure network becomes a new functionality: besides the fluid flow it can transfer heat by propagating temperature along the "temperature wires".

In the example shown in Figure 2(a) the power is injected to the extended pressure network at fluid nodes FN1 [...] FN4 located inside of the transformer coil. The power generated in the winding segment between fluid nodes FN1 and FN2 (see Figure 2(b)) is distributed to both nodes according to the mass flow rate in the corresponding cooling ducts. In this case the extended pressure network acts as a parallel carrier for the power flow and ensures the correct balance between convection, conduction and radiation inside the winding. The fluid nodes FN5-FN7 are used for both heating and cooling. Thermal networks including the transformer core, the additional eddy losses as well as the tank walls and cover cooling capacities are attached to these nodes. Whether the fluid is heated or cooled at these nodes depends on characteristics of the specific transformer design. The last fluid node FN8 is removing the heat from the fluid according to the radiators cooling model.

In a closed cooling loop as shown in system like in Figure 2(a) the sum of the power injected and removed to/from all fluid nodes must be zero (a nonzero value obtained as a solution of the network model is a measure of numerical error). For solving of the coupled network we use the Spice solver designed for electrical networks (Quarles *et al.*, 1993). The thermal and pressure networks can be also solved with Spice by applying analogies between the network quantities summarized in Table I.

3. Definition of network elements

3.1 "Branch" and "Node" elements

The internal schemes of the "Branch" and "Node" elements are shown in Figure 3.

The thermal resistance R_{flow} connects the internal node at inlet temperature with the fluid node at average branch temperature ϑ_{FN}. Assuming linear temperature distribution along the "Branch" we calculate ϑ_{FN} as follows[1]:

$$\vartheta_{FN} = \frac{\vartheta_{inlet} + \vartheta_{outlet}}{2} \tag{2}$$

Based on (1) with $\Delta\vartheta = \vartheta_{outlet} - \vartheta_{inlet}$ and (2) we define R_{flow} as:

$$R_{flow} = \begin{cases} \frac{1}{2\lvert\dot{m}\rvert c_p} \; if \lvert\dot{m}\rvert \geq \dot{m}_{tol} \\ \frac{1}{2\dot{m}_{tol} c_p} \; if \lvert\dot{m}\rvert < \dot{m}_{tol} \end{cases} \tag{3}$$

where $\dot{m}_{tol}$ is the mass flow rate tolerance that prevents from discontinuity of the network for infinite value of R_{flow}.

		Extended pressure network	
Electric network	Thermal network	Temperature wires	Fluid flow wires
Current (A)	Power (W)	–*)	Mass flow rate (kg/s)
Voltage U (V)	Temperature (°C)	Temperature (°C)	Pressure (Pa)
Electric resistance (Ohm)	Thermal resistance (K/W)	–*)	Flow resistance (1/(m*s))

Table I.
Analogy between quantities and units of electric, thermal and pressure networks

Notes: *)There is no "current" in the temperature wires of the pressure network. These wires transfer the "temperature signal" only. The direction of this transfer is the same as the direction of the fluid flow

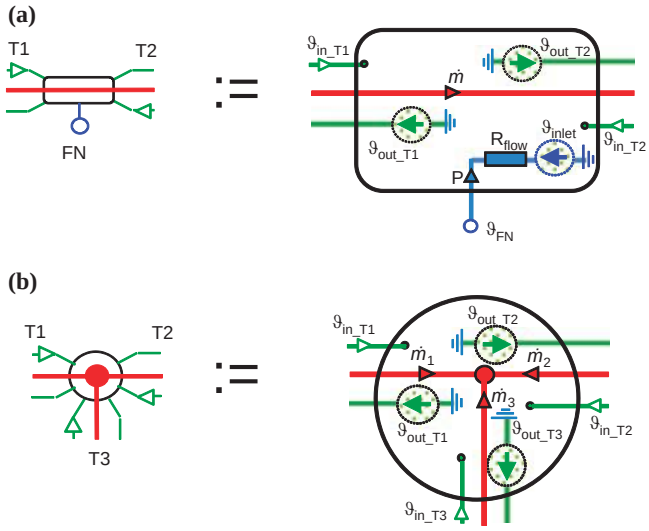

Notes: Each terminal denoted as T1, T2, T3 consists of two temperature pins (input and output) and one pressure network pin. The pins with the green arrow at each terminal represent the temperature input while the pin without arrow is an output pin. When connecting two pins it is required that the input pin is connected to the output pin of another element and vice versa. This ensures that the direction of temperature propagation within each network branch is consistent (as shown in Figure 2(a))

Figure 3.
Networks representation of (a) "Branch" and (b) "Node" elements

In general case the inlet and outlets of "Branch" elements are not known. Their location is determined by the solution of the pressure network. Consequently, we have to calculate the ϑ_{inlet} and ϑ_{outlet} as a function of the mass flow rate direction $\dot{m}$ (the positive direction of $\dot{m}$ is from the terminal T1 to the terminal T2 as shown in Figure 3(a)):

$$\vartheta_{inlet} = \begin{cases} \vartheta_{in\_T1} & if\ \dot{m} \geqslant 0 \\ \vartheta_{in\_T2} & if\ \dot{m} < 0 \end{cases} \tag{4}$$

$$\vartheta_{outlet} = \vartheta_{inlet} + 2R_{flow}P \tag{5}$$

The direction of power P determines whether the fluid is heated or cooled. The positive direction of P corresponding to heating is defined as the direction towards the "Branch" (see Figure 3(a)).

Formally, ϑ_{outlet} must be defined only for one temperature output pin that corresponds to the direction of the mass flow. The other output pin is not used for propagation of the temperature signal. However, in order to ensure the consistency of the network the unused output pins are set to the temperature of the input pin connected to the same terminal of the "Branch" element:

$$\vartheta_{out\_T1} = \begin{cases} \vartheta_{inlet} & if\ \dot{m} \geqslant 0 \\ \vartheta_{outlet} & if\ \dot{m} < 0 \end{cases} \quad \vartheta_{out\_T2} = \begin{cases} \vartheta_{outlet} & if\ \dot{m} \geqslant 0 \\ \vartheta_{inlet} & if\ \dot{m} < 0 \end{cases} \tag{6}$$

Based on (6) we ensure that both temperature pins at each terminal have always the same temperature independent of the direction of the fluid flow. This feature enables correct referencing of temperatures by other network elements before the flow direction is known.

The output temperature of the "Node" is defined as an average temperature of incoming fluids weighted by the product of $|\dot{m}|c_p$ according to (1):

$$\vartheta_{mixed} = \frac{\sum_{\dot{m}_j > 0} \dot{m}_j c_{pj} \vartheta_{in\_j}}{\sum_{\dot{m}_j > 0} \dot{m}_j c_{pj}} \tag{7}$$

Similar to output pins of the "Branch" element the unused output pins of the "Node" (at terminals i of incoming flow) are set to the corresponding input temperature to ensure consistency of temperatures across the network:

$$\vartheta_{out\_i} = \begin{cases} \vartheta_{in\_i} \, if \, \dot{m}_i \geqslant 0 \\ \vartheta_{mixed} \, if \, \dot{m}_i < 0 \end{cases} \tag{8}$$

Both "Branch" and "Node" do not include any elements of the pressure network. They have to be included into the extended pressure network separately as specified in the next subsection. The role of "Branch" and "Node" as well as the topology of the network between them is to provide a consistent mechanism of temperature propagation that creates a backbone for the coupled network.

3.2 Pressure network elements

For the forced cooling the main excitation of the fluid flow is provided by devices like pumps, compressors or ventilators. Their volume flow characteristics $\dot{V}(\Delta p)$ are used to calculate the mass flow rate $\dot{m}_{forced}$, which is included in the pressure network as a "current source":

$$\dot{m}_{forced} = \rho \cdot \dot{V}(\Delta p) \tag{9}$$

where ρ is the fluid density and Δp the pressure drop on the pump.

For natural convection the main excitation in the network results from the buoyancy. It is introduced to the network as a buoyancy pressure head Δp_{bh} represented by a "voltage source":

$$\Delta p_{bh} = gH\left(\rho_{ref} - \rho\right) \tag{10}$$

where g is the gravitational acceleration, H the pressure height (height of the equivalent fluid column), ρ_{ref} and ρ the fluid mass densities for the reference and average fluid temperatures, respectively.

Other pressure drops are defined in the following form:

$$\Delta p = \frac{1}{2} \xi \rho v^2 \tag{11}$$

where v is the velocity of the fluid and ξ the pressure drop coefficient. Equation (11) is implemented directly as a "voltage source" (like buoyancy head) only for cases where the velocity v as well as the pressure drop Δp are defined in different branches

(Nakadate *et al.*, 1996). A more typical way of introducing pressure drops offer the flow resistance S_{flow}. It is calculated as the ratio between pressure drop and the mass flow rate (both in the same network branch) and can be expressed by using (11) as follows:

$$S_{flow} = \frac{\Delta p}{\dot{m}} = \frac{1}{2}\frac{\xi}{\rho A_c^2}|\dot{m}| \tag{12}$$

where A_c is the duct cross-section area. The pressure drop coefficient ξ depends on the components of the Bernoulli equation that are relevant for the selected flow model. As an example (used for liquid-filled transformers) we present here the flow loss coefficient resulting from the inner friction of the fluid in case of non-fully developed laminar flow through a planar duct (Rohsenow *et al.*, 1998):

$$\xi = \frac{4}{\mathrm{Re}}\frac{L}{D_h}\left(\frac{3.44}{(x^+)^{1/2}} + \frac{24 + 0.674/(4x^+) - 3.44/(x^+)^{1/2}}{1 + 0.000029(x^+)^{-2}}\right) \quad \text{With} \quad x^+ = \frac{L}{D_h \mathrm{Re}} \tag{13}$$

and the Reynolds number:

$$\mathrm{Re} = \frac{D_h \cdot \mathrm{v}}{\nu} \tag{14}$$

where L is the duct length, D_h the hydraulic diameter of the flow, v the average fluid velocity and ν the kinematic viscosity of the fluid at average temperature.

3.3 Thermal network elements

The formulation of thermal network elements has been a subject of comprehensive research work performed in the past. The corresponding definitions can be found in the literature (Gramsch *et al.*, 2007; Loebl, 1984; Holman, 1999).

However, the coupled network concept may imply a slightly different approach when defining the convection resistors representing the heat transfer through the boundary layer. As an example we present here the convection resistance R_{conv} for a non-fully developed laminar flow in a planar duct (Rohsenow *et al.*, 1998):

$$R_{conv} = \frac{1}{hA} \text{ with heat transfer coefficient } h = \frac{Nuk_f}{D_h} \tag{15}$$

and with the Nusselt number:

$$Nu = 8.235 + \frac{0.024(x^*)^{-1.14}}{1 + 0.0358\,\mathrm{Pr}^{0.17}(x^*)^{-0.64}} \text{ with } x^* = \frac{L/D_h}{\mathrm{Re}\,\mathrm{Pr}} \tag{16}$$

where A is the heat transfer area, Pr the Prandtl number and k_f the thermal conductivity of the fluid, both evaluated at average duct temperature. See (13) and (14) for definition of other quantities.

The resistor defined by (15) and (16) can be used not only for the forced but also for the natural convection. The velocity required for evaluation of the Reynolds number can be obtained in both cases thanks to the coupling with the pressure network. It is essential that the convection resistors used in a coupled thermal network are focused on boundary layer representation and do not include empirical correction factors introduced due to fluid flow.

4. Solution method

4.1 Separation of networks

The coupled network problems are difficult to solve using the Newton-Raphson method implemented by Spice. Therefore, we have split the coupled network into two separate networks and solve them iteratively[2]. The first network, pure pressure one, consists of the fluid flow branches including all flow resistances, buoyancy heads and pumps. The second one consists of the whole thermal network and the temperature branches of the extended pressure network. The "Branch" and the "Node" elements are the only network components that have a separate representation dedicated for each of the two networks. The separated networks can be solved using Spice by assuming boundary conditions in form of interface variables that are iteratively delivered by the solution of the other network. These interface variables include mass flow rates and velocities as a solution $x_p \in \mathbb{R}^m$ of the pure pressure network as well as temperatures as a solution $x_t \in \mathbb{R}^n$ of the thermal/temperature network, with n, m being the number of the corresponding interface variables.

The global solution is then computed by fixed-point iteration. In every step of the iteration, we have to solve two individual networks – the thermal and the pressure. Let the subscript i be the current iteration step number, f_p: $\mathbb{R}^m \mapsto \mathbb{R}^n$ the function to compute a solution x_t of the thermal and f_t: $\mathbb{R}^n \mapsto \mathbb{R}^m$ a solution x_p of the pressure network. We can then write the fixed-point iteration to solve the global problem as:

$$\begin{aligned} x_{p,i} &= f_p\left(x_{t,i}\right), x_{t,i} \in \mathbb{R}^n, x_{p,i} \in \mathbb{R}^m, i = 0, 1, 2, \ldots \\ x_{t,i+1} &= f_t\left(x_{p,i}\right) \end{aligned} \tag{17}$$

or in a more compact way:

$$x_{t,i+1} = f_t\left(f_p\left(x_{t,i}\right)\right), \; x_{t,i} \in \mathbb{R}^n, i = 0, 1, 2, \ldots$$

Before starting iterations the initial solution $x_{t,0}$ of the thermal network must be specified. This is typically done based on rough engineering formulas for temperature calculations (Figure 4).

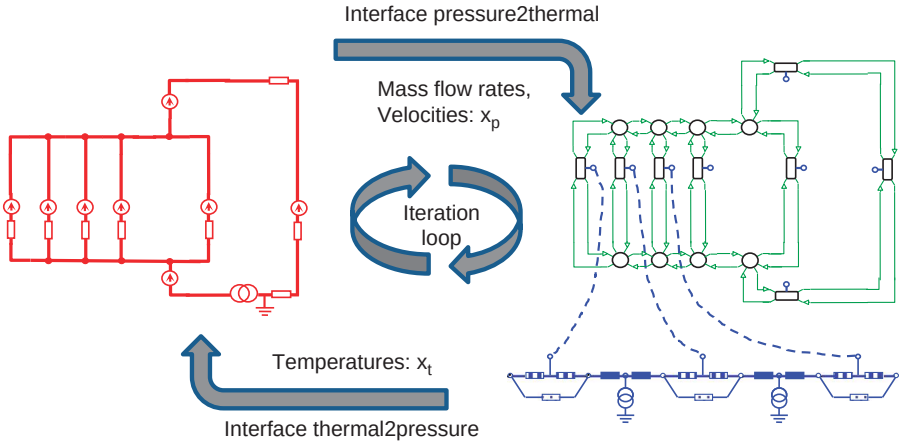

Figure 4.
Splitting networks for iterative solution

Note: The convergence criterion requires that for all interface variables the relative change between subsequent iterations (relative error) is less than a predefined value

4.2 Adaptive relaxation

To ensure convergence and reduce the number of required iterations, we apply a relaxation technique to the computed interface variables of both networks. The result x_t or x_p of the network solution is not used as is, but instead the difference between the new and the previous result is calculated. Then, a fraction of this difference is added to the previous result to make a step in the direction of the new result, which creates the relaxed solution x'_t or x'_p, respectively. The length of this step is controlled by the relaxation factors Δ_t, $\Delta_p \in (0;1]$.

Using f'_t and f'_p to denote the relaxed solution of the network computation f_t and f_p, respectively, we can rewrite equation (17) as relaxed fixed-point iteration:

$$\begin{aligned} &x'_{t,i+1} = f'_t\left(x'_{t,i}, x'_{p,i}\right) \\ &x'_{p,i+1} = f'_p\left(x'_{t,i+1}, x'_{p,i}\right), \quad x'_{t,i} \in \mathbb{R}^n, x'_{p,i} \in \mathbb{R}^m, \quad i = 0,1,2,\ldots \\ &\text{with} f'_t\left(x^i_{t,i}, x^i_{p,i}\right) := x'_{t,i} + \Delta_{t,i} * \left(f_t\left(x'_{p,i}\right) - x'_{t,i}\right), \text{ and } f'_p \text{ accordingly} \end{aligned} \tag{18}$$

The convergence towards a fixed point x^* is affected by the spectral radius ρ_s of the Jacobian matrix at the fixed point. If $\rho_s < 1$, the iteration will converge to the fixed point x^* for a suitably chosen starting point x_0. The smaller values of ρ_s usually result in a faster convergence rate (Ortega and Rheinboldt, 1970; Berinde, 2007). The relaxation factors Δ_t, Δ_p have a direct influence on ρ_s and the convergence behaviour. The details are explained in a case study presented in the Appendix.

The relaxation factors Δ_t, Δ_p are handled separately for both networks and are adapted during the iteration using the constant increase, respectively, decrease factors $C_{inc} \geqslant 1.0$ and $C_{dec} \in (0;1]$ depending on the previous results of the corresponding network:

$$\Delta_{t,i+1} := \begin{cases} \Delta_{t,i} * C_{inc}, & \left\| x'_{t,i-1} - x'_{t,i} \right\|_2 < \left\| x'_{t,i-2} - x'_{t,i-1} \right\|_2, \text{and } \Delta_{p,i+1} \text{ accordingly} \\ \Delta_{t,i} * C_{dec}, & \text{otherwise} \end{cases} \tag{19}$$

Additionally, we impose both an upper and lower limit to the relaxation factors. At the beginning of the iteration the admissible interval is $[C_{min}; C_{max}]$. To ensure that the relaxation factors are gradually reduced and to prevent large jumps at high iteration counts i, the interval is adjusted during iterations. Both upper and lower limit are steadily reduced by factor δ_i to 50 per cent of their initial value:

$$[\delta_i * C_{min}; \delta_i * C_{max}], \quad \text{with } \delta_i := \left(1.0 - \frac{0.5 * i}{C_{MaxIterCount}}\right) \tag{20}$$

Furthermore, in every iteration step heuristic rules may be applied to decrease Δ_t or Δ_p in order to avoid or mitigate known convergence obstacles, such as excessive/unrealistic values (e.g. large temperature jumps) or flow direction changes (see next subsection). However, this decrease is only used in the specific iteration step and is ignored during computation of the relaxation factor for the next iteration.

Even though the relaxation is realized in a very straight forward way, the results are promising, as Figure 5(c) shows. Nevertheless, more complex mechanisms such as, e.g. vector extrapolation methods (Jbilou and Sadok, 2000) could be used in future.

4.3 Flow direction change control

The network branches with a small mass flow rate show a tendency to change the flow direction during the iterative solution. Due to the significant temperature difference between the top and bottom fluid the direction changes may lead to non-convergence. For the vertical coil ducts this problem can be mitigated by disabling the flow from the top to the bottom by means of "blocking" resistors (acting similar to a diode). However, such a flow control method cannot be applied to arbitrary bidirectional flows. Therefore, we apply an enhanced relaxation that decreases the value of Δ_p to a minimum level, which ensures no direction change of any interface variable in x_p (just one most critical result decides about Δ_p). The corrected value of Δ_p sets one of the mass flow rate or velocity results to zero while all other ones keep the same direction. In the next iteration step the variable that has been set to zero is free to change in any direction while the other ones are still controlled by the enhanced relaxation.

An example of the convergence behaviour with enhanced relaxation due to flow direction change has been presented in Figure 5(d). A comparison of this result with the corresponding result in Figure 5(c) shows that the efficiency of the enhanced relaxation is equivalent to applying blocking resistors. However, the latter one can be used only for the *a priori* known flow direction. Otherwise, the enhanced adaptive relaxation offers more robustness in solving bidirectional flow problems as presented in the next section.

5. Bidirectional flows. "Hotspot" model

5.1 Problem formulation and modelling approach

Another example related to a guided fluid flow in a transformer disk winding is shown in Figure 6. By selecting an optimum configuration of "guides" forcing the flow into the horizontal ducts between disks a better cooling of the winding can be achieved. Such a detailed model is used by transformer designers for identification of the hottest disk in the winding and is called the "hotspot" model.

In order to efficiently create a network model we have applied a technique similar to integrated circuit modelling (see Figure 7). This kind of guided duct representation can be included in a full model of a transformer shown in Figure 2(a) by replacing one of winding flow branches with the collection of stacked sub-circuits (the connections at the bottom and the top of the stacked model are compatible with the "Nodes"). Alternatively, the detailed model from Figure 7 can be solved separately by applying boundary conditions in form of mass flow rate and the bottom fluid temperature. Typically, the values of the boundary conditions can be obtained from a computation of the full transformer model using a simplified, averaged winding representation as shown in Figure 2. These values can be passed not only to a detailed network model but can be also used as boundary conditions in a CFD computation, which enables a comparison between both approaches. The values of the boundary conditions as well as the considered guide configurations (cases 1 and 2) are specified in Figure 6.

5.2 Results and comparison with CFD

The results for two configurations of the "hotspot" model are shown in Figure 8. The first one (case 1) is a typical configuration used in transformer winding design. For natural convection, which has been implicitly assumed here by prescribing a low

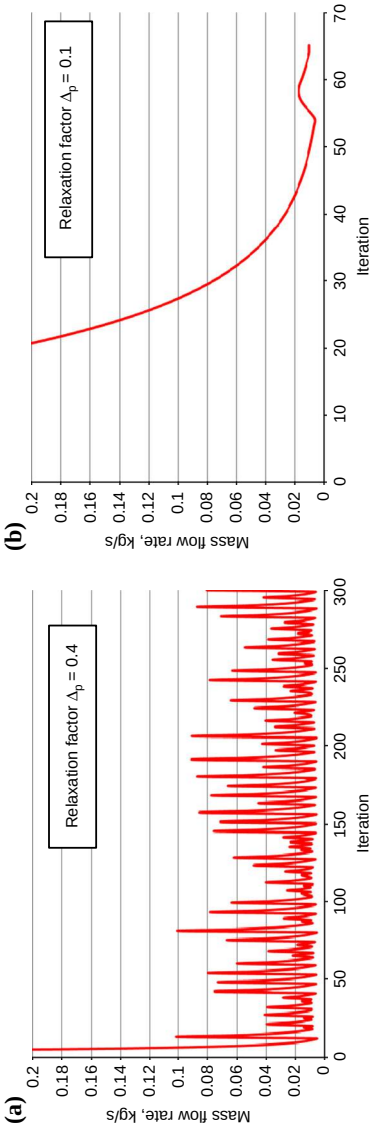

Notes: We selected from the arrangement in Figure 1 a duct transporting a relatively small fraction of the total heat power (<0.5 per cent). Consequently, up to 40 iterations are needed to converge (c, d). Other load cases of the same transformer with larger or zero heat power transported through the same duct converge within ten to 20 iterations. Constant relaxation factors may lead to non-convergence (a) or require considerably more computational effort (b)

Figure 5.
Convergence behaviour of mass flow rate in a liquid transformer coil cooling duct calculated for different relaxation approaches

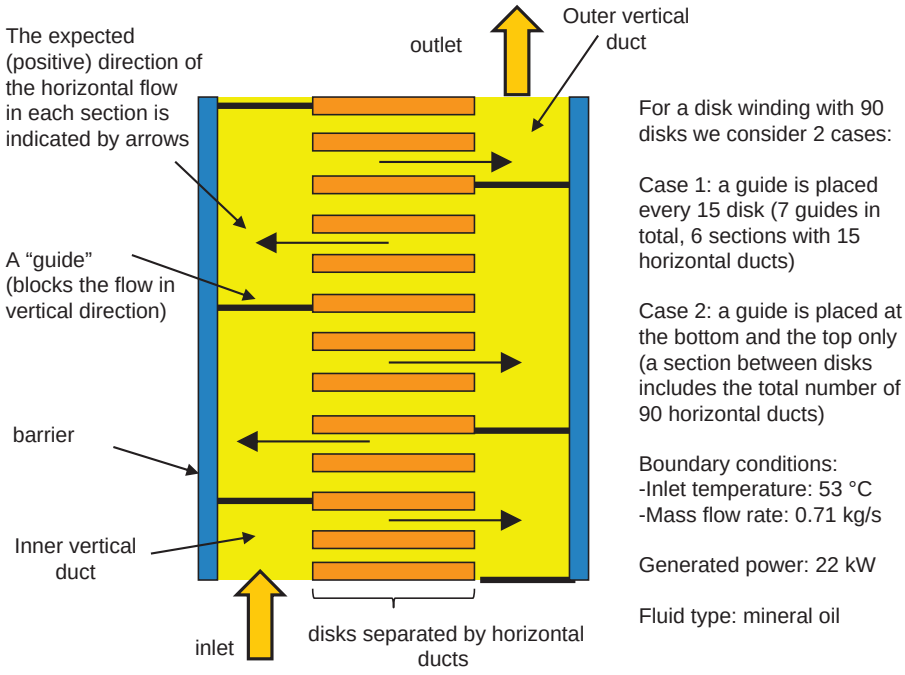

Figure 6.
Transformer disk winding with guided flow

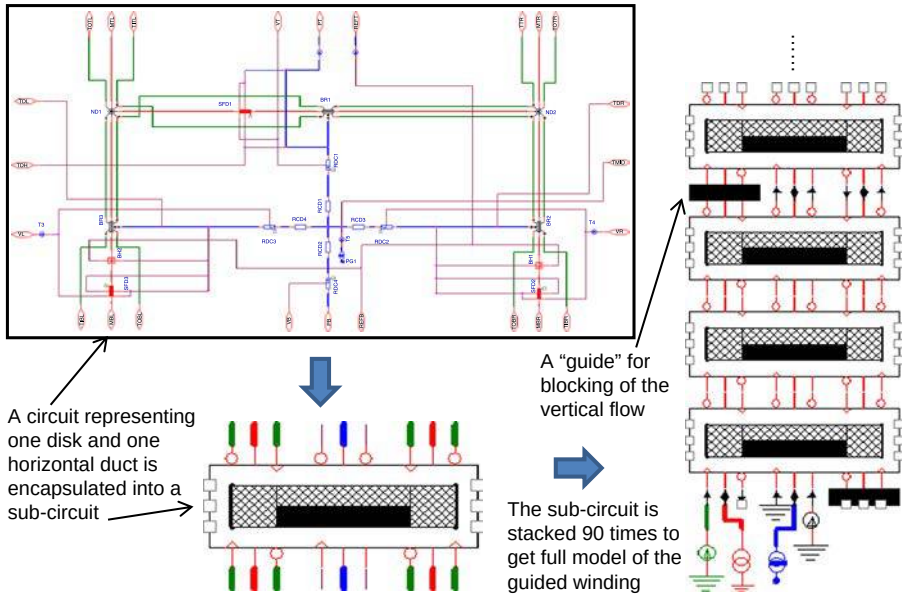

Figure 7.
Network model of a guided transformer disk winding created with the electronic circuits design program Capture/OrCAD

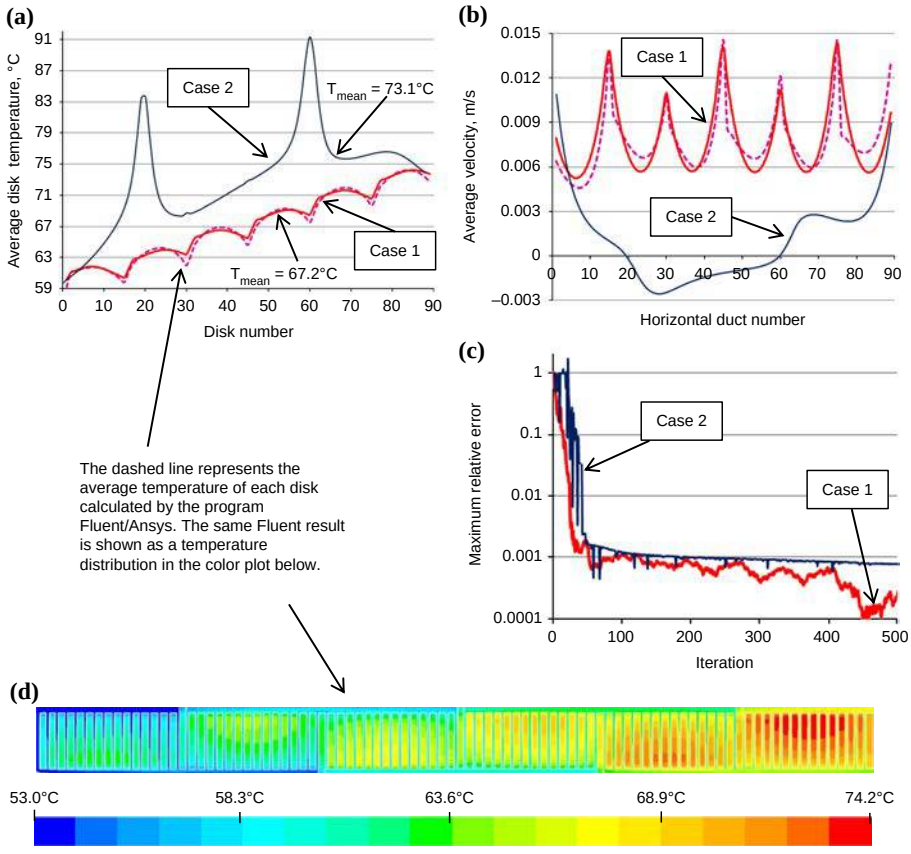

Notes: (a) Average temperature distribution from the bottom disk to the top; (b) average velocity for horizontal ducts from the bottom to the top; (c) convergence behavior of the relative error during iterations; (d) color plot of temperature distribution in the disk winding calculated with CFD

Figure 8.
Results of flow computations in a transformer disk winding for "case 1" with seven guides and for "case 2" with two guides

value of the mass flow rate, a regular pattern of the temperature distribution has been obtained (see Figure 8(a) and case 1). Also the flow in horizontal ducts behaves as expected, which is confirmed by positive values of the velocity (in expected direction) (see Figure 8(b) and case 1). The regular pattern of both distributions enables the creation of simplified averaged models to be applied in a network for a full transformer. The guided flow for case 1 shows a good convergence behaviour that requires less than 50 iteration steps to achieve the desired error level of 0.001 (Figure 8(c)).

The comparison with CFD analysis shows an acceptable agreement, see dashed lines in Figure 8(a), (b) and color plot in Figure 8(d). The deviation of average temperature calculated for all disks using CFD and network models is 0.2 K while the standard deviation resulting from comparison of local disk temperatures is 0.4 K. This range of accuracy is sufficient for technical applications. It should be noted that the network and CFD models used for comparisons are not exactly the same. In order to enable equivalent 2D CFD computations the sticks placed in the cooling ducts have

to be removed from the CFD computation and instead correction factors for boundary conditions and input parameters have to be applied, while the coupled network is geometrically by default a 3D model.

The results for case 2 show that the flow in horizontal ducts is changing direction within the big section between the top and bottom as indicated by the negative velocity in Figure 8(b). At the locations where the horizontal velocity is close to zero the highest disc temperatures (hotspots) have been calculated (see Figure 8(a)). However, one should be careful with the quantitative evaluations since the solution is very sensitive to changes of input data. Small deviations related to manufacturing tolerances may contribute to a significant change of the hotspot value and location. In addition, the convergence behaviour shown in Figure 8(c) indicates that the relative error is decreasing slower for case 2 than for case 1 and stagnates at a certain level. But also, the corresponding CFD computation for case 2 behaves unstable: fluctuations of the residual value monitored in the CFD iteration process have been observed. The quantitative evaluation of such non-guided flows (including their transient behaviour) as well as their numerical characteristics (like spectral radius) are still a subject of further research for both CFD (Jiao, 2012) and network approaches. Therefore, we present here only the network result for case 2 in order to illustrate that the new solution method described in Section 4 is able to handle a serious discontinuity, which is the flow direction change and zero velocity in horizontal ducts.

6. Conclusion

The new concept of coupled networks and the proposed solution method have been implemented as a computational tool for a new transformer design system. The first evaluations confirmed that the required level of accuracy can be improved compared with the traditional computation method. In addition, the new tool offers a reliable convergence behaviour as well as robustness in creating new transformer configurations. Comparing with CFD the coupled network approach shows better performance characteristics that allows interactive use in an engineering design system. The computation of a full transformer model with averaged representation of cooling ducts takes a few tens up to a few hundred milliseconds on a standard notebook computer. This enables its application in optimization jobs that require hundreds or thousands of computations. The detailed "hotspot" computations can be accomplished within a few seconds for well converging models. Therefore, the coupling of pressure and thermal networks offers a good alternative to the CFD approach, in particular for engineering computations where the streamlines of the flow are known and the topology of the extended pressure network can be created.

Notes

1. The assumption of linear temperature distribution between inlet and outlet may be questionable for temperature-imposed behavior of the thermal network connected to the fluid node. A typical example is a resistor representing cooling capacity of the whole radiator for a specified reference temperature (connected to the fluid node FN8, Figure 2a). Such a simplified model may result in radiator outlet temperature that is lower than the ambient. A solution of the problem may require more complex network models as presented in Olsson (2012). However, a piecewise linear approximation based on dividing the single "Branch" element into a few ones allows to achieve a logarithmic distribution of the temperature along the radiator.
2. The iterative solver performs the splitting automatically based on a naming convention for extended pressure network elements and their pins.

References

Berinde, V. (2007), *Iterative Approximation of Fixed Points*, Springer, Berlin, NY.

Gramsch, C., Blaszczyk, A. and Löbl, H. (2007), "Thermal network method in the design of power equipment", *SCEE Conference Book (ISBN 978-3-540-71979-3)*, Springer Verlag, Heidelberg.

Holman, J.P. (1999), *Heat Transfer*, 8th ed., McGraw-Hill, New York, Singapore.

Jiao, Y. (2012), "CFD study on the thermal performance of transformer disc windings without oil guides", MSc thesis, Royal Institute of Technology, Stockholm.

Jbilou, K. and Sadok, H. (2000), "Vector extrapolation methods. Applications and numerical comparison", *Journal of Computational and Applied Mathematics*, Vol. 122 Nos 1-2, pp. 149-165.

Loebl, H. (1984), "Zur Dauerstrombelastbarkeit und Lebensdauer der Geräte der Elektroenergieübertragung", Dissertation B, Dresden, Saxony.

Nakadate, M., Toda, K., Sato, K., Biswas, D., Nakagawa, C. and Yanari, T. (1996), "Gas cooling performance in disc winding of large-capacity gas-insulated transformer", *IEEE Trans. On Power Delivery*, Vol. 11 No. 2, pp. 903-908.

Olsson, C.O. (2012), "Buoyancy driven flow in counter flow heat exchangers", *Paper 3475, 6th European Thermal-Sciences Conference, 4-7 September, Poitiers*.

Ortega, J. and Rheinboldt, W. (1970), *Iterative Solution of Nonlinear Equations in Several Variables*, Academic Press, New York, NY.

Quarles, T., Newton, A.R., Pederson, D.O. and Sangiovanni-Vincentelli, A. (1993), *Spice 3 Version 3f3 User's Manual*, University of California, Berkeley, CA.

Rohsenow, W.M., Hartnett, J.P. and Cho, Y.I. (1998), *Handbook of Heat Transfer*, McGraw-Hill, New York, NY.

Appendix

Case study on convergence behaviour of a simplified heater-cooler circuit

The purpose of this study is the creation of a simplified and linerized network model according to the principles explained in Sections 2 and 3 in order to perform a theoretical analysis of the convergence behaviour. We use two variants of a simple circuit with a heating and a cooling device connected into a pressure network loop. The first variant with one heated duct (Figure A1) presents the elementary analytical solution while the second one (Figure A3) with two heated ducts allows to make conclusions on how the fluid flow splitting influences the convergence characteristics of more complex devices like transformers.

According to (18) the relaxed version of thermal and pressure equations for the one-duct model can be written as follows:

$$\Delta\vartheta'_{i+1} = \Delta\vartheta'_i + \Delta \cdot \left(\frac{B}{\dot{m}_i} - \Delta\vartheta'_i\right)$$

$$\dot{m}'_{i+1} = \dot{m}_i + \Delta \cdot \left(\frac{\Delta\vartheta'_{i+1}}{2A} - \dot{m}'_i\right) \tag{A21}$$

where Δ is the relaxation factor (same for both equations), while A and B are constants defined in Figure A1. The iteration process is illustrated in Figure A2(a). The spectral radius of the Jacobian matrix at the fixed point of the equation system (21) has been calculated analytically and the result is shown in Figure A2(b). It can be seen that for the unrelaxed iteration ($\Delta = 1$) the $\rho_s = 1$ and therefore it does not converge. The lowest spectral radius has been obtained for $\Delta_{opt} = 0.828$, which provides the fastest convergence rate. For $\Delta = 0.828$ the number of iterations required to fulfil the convergence criterion (relative change of both variables < 0.001) is equal 6 in contrast to 11 iterations required for $\Delta = 0.5$ as shown in Figure A2(a).

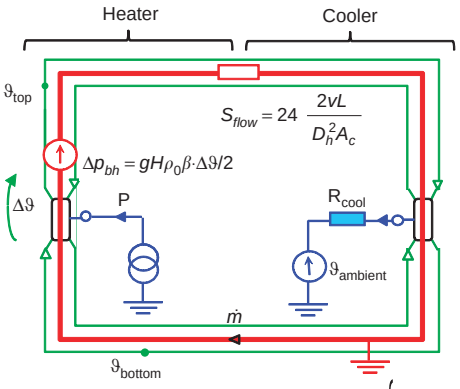

Assumptions:

- Pressure head Δp_{bh} (10) is based on linear dependency of density from temperature: $\rho = (1-\beta\vartheta)\rho_0$
- The flow resistance S_{flow} is valid for laminar, fully developed flow: with $x^+ \to \infty$ in (12),(13)
- R_{cool} and fluid properties are temperature independent. The average fluid temperature $(\vartheta_{top}+\vartheta_{bottom})/2$ does not affect the mass flow. The problem can be reduced to two unknowns $\Delta\vartheta = \vartheta_{top}-\vartheta_{bottom}$ and $\dot{m}$ with the following equations:

Pressure equation: $\Delta\vartheta = 2\,\frac{S_{flow}}{gH\rho_0\beta}\,\dot{m} = 2A\dot{m}$

Thermal equation: $\Delta\vartheta = \frac{P}{c_p}\frac{1}{\dot{m}} = B\,\frac{1}{\dot{m}}$

The physically valid fixed point: $\{\Delta\vartheta, \dot{m}\} = \left\{\sqrt{2AB}, \sqrt{\frac{B}{2A}}\right\} = \{15.64, 3.20\}$

Figure A1.
A heater-cooler circuit with one heated duct based on natural convection

Notes: The geometrical dimensions, boundary conditions and the linearized fluid properties are defined in Section 3. The values (representative for a small power transformer) are as follows: P = 100 kW, D_h = 10 mm, A_c = 0.25 m^2, L = 3 m (including the cooler and the heater ducts), H = 1 m (H is interpreted as the "thermal head", which is the height difference between the "thermal center" of the cooler and the "thermal center" of heater), ν = 3e-6 m2/s, ρ_0 = 900 kg/m^3, β = 8e-4 1/K, c_p = 2000 J/kg/K

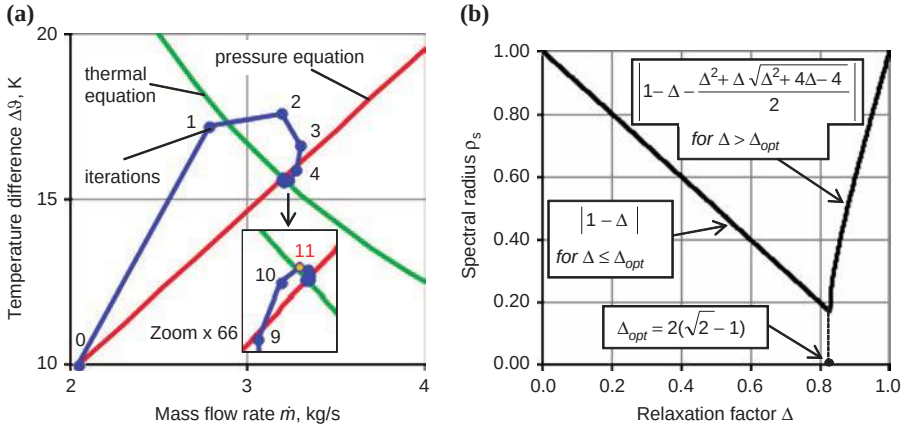

Figure A2.
Results for the one-duct heater-cooler circuit in Figure A1

Note: (a) Fixed-point iterations for Δ = 0.5 and $\Delta\vartheta_0$ = 10 K, (b) spectral radius ρ_s as a function of relaxation factor Δ

A two-duct variant of the heater defined in Figure A3 shows dependence of the convergence rate from the fraction of power injected into each duct. An example of fixed point iterations for the heated ducts with a large and a small power split fractions ($k_s = 0.5$ and $k_s = 0.005$) as well as the results of numerical analysis of the spectral radius are shown in Figure A4. It is evident that the duct with 0.5 per cent of power requires significantly more iterations than the other duct and the relaxation factor must be < 0.33 to converge. This result explains the non-convergence case shown for a similar real transformer in Figure 5(a) with $\Delta = 0.4$.

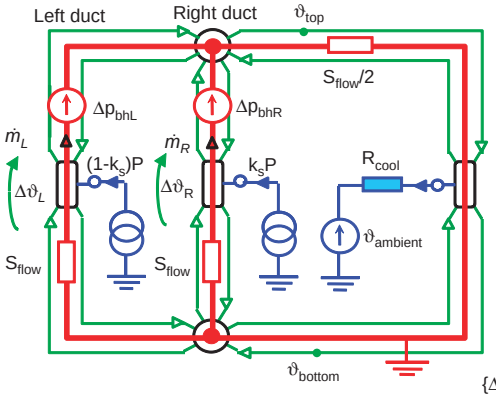

Pressure equations (valid for $\dot{m}_L > 0$, $\dot{m}_R > 0$):

$$\Delta\vartheta_L = A(3\dot{m}_L + \dot{m}_R)$$

$$\Delta\vartheta_R = A(\dot{m}_L + 3\dot{m}_R)$$

Thermal equations:

$$\Delta\vartheta_L = (1 - k_s)B\frac{1}{\dot{m}_L}$$

$$\Delta\vartheta_R = k_sB\frac{1}{\dot{m}_R}$$

The fixed point values for k_s=0.5:

$\{\Delta\vartheta_L, \dot{m}_L, \Delta\vartheta_R, \dot{m}_R\} = \{15.64, 1.60, 15.64, 1.60\}$

The fixed point values for k_s=0.005:

$\{\Delta\vartheta_L, \dot{m}_L, \Delta\vartheta_R, \dot{m}_R\} = \{19.15, 2.60, 6.63, 0.0377\}$

Notes: This model has the same parameters as the one-duct model in Figure 9. For k_s=0.5 the fixed-point values correspond to the one-duct fixed point values

Figure A3.
Heater-cooler circuit with two heated ducts

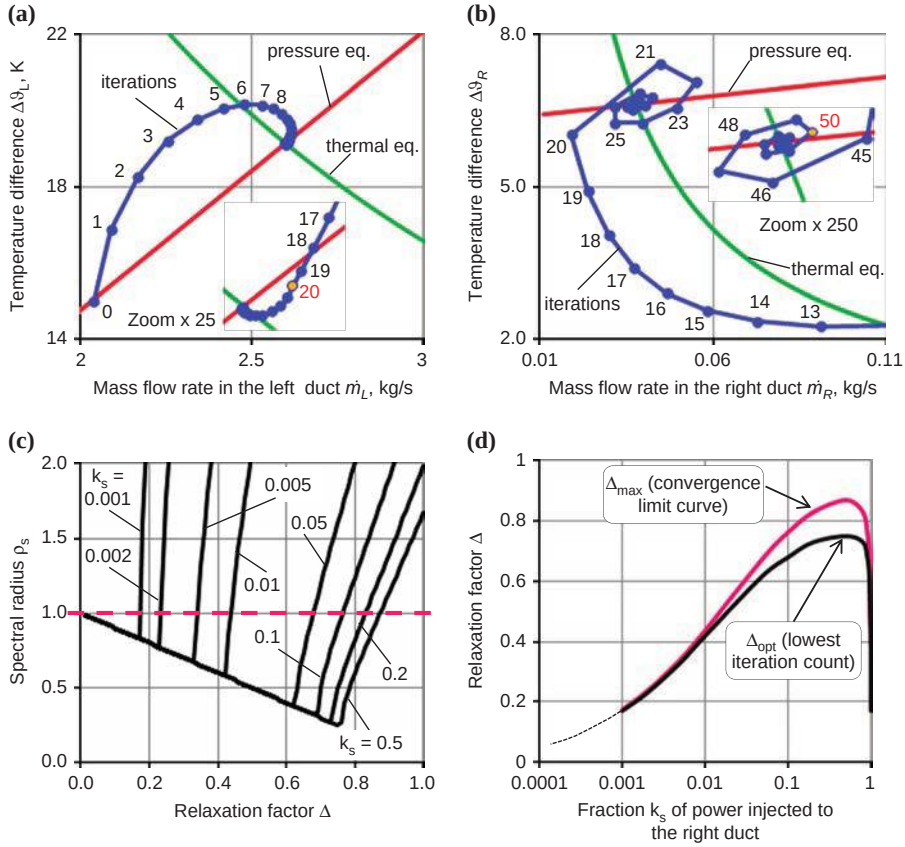

Figure A4.
(a) and (b) Results of fixed point iterations in the two-duct model from Figure A3 calculated for $k_s = 0.005$, $\Delta = 0.2$ and $\Delta\vartheta_{L0} = \Delta\vartheta_{R0} = 15$ K; (c) the spectral radius calculated numerically for different k_s values; (d) relationship between the maximum and the optimum relaxation factors and power fraction k_s (all combinations $\{\Delta, k_s\}$ above the upper curve will not converge)

The relationship between the relaxation factor Δ and the power split fraction k_s shown in Figure A4(d) is an important result of the spectral radius analysis. It allows making direct conclusions for selection of the constants C_{max} and C_{min} used in the adaptive relaxation algorithm presented in Section 4.2. It confirms our strategy of reducing Δ adaptively from 0.8 to 0.01. However, in real cases the solution is reached before reducing Δ to 0.01 since for very small values of k_s the convergence is ensured by selecting an appropriate mass flow tolerance that stabilizes the value of thermal resistance in the Branch elements (3).

About the authors

Dr Andreas Blaszczyk was born in Bytom, Poland, in 1955. In 1979 and 1984 he received his Diploma and PhD Degree in Electrical Engineering from the Silesian Technical University Gliwice, Poland where he continued to work on simulation of electric power systems until 1987. From 1988 he was a Researcher at the Technical University Munich in the area of simulation of electric fields in high voltage engineering. In 1990 he joined ABB Corporate Research in Heidelberg/Germany and in 2003 he switched within the same organization to Baden/Switzerland. His research work at ABB includes dielectric, thermal and electromechanical simulation of power devices as well as the high performance computing. Dr Andreas Blaszczyk is the corresponding author and can be contacted at: Andreas.Blaszczyk@ch.abb.com

Dr Reto Flückiger was born in 1978 in Rheinfelden, Switzerland. He received his Diploma in Mechanical Engineering in 2004 from ETH Zurich. Afterwards he worked as a Research Assistant at the Zurich University of Applied Science on high temperature fuel cell simulations. Between 2006 and 2009 he made his PhD on low temperature fuel cells with the Paul Scherrer Institute in Switzerland. Since 2009, he has been working at ABB Switzerland – Corporate Research on the thermal management of power products.

Dr Thomas Müller was born in Munich, Germany, in 1983. He received his Diploma in Mathematics from the Technische Universität München in 2008 and is currently working at the same university as a Research Assistant with the Chair for Computer Architecture at the Department of Informatics. His PhD, accomplished in 2014, is in the area of Industrial Simulation Software on Multi- and Many-Core Architectures and has been carried out in close cooperation with Corporate Research of ABB Schweiz AG.

Dr Carl-Olof Olsson, born 1969 in Sweden, graduated in Mechanical Engineering in 1992 and received a PhD in thermo and fluid dynamics in 1997 from the Chalmers University of Technology in Göteborg, Sweden. He joined the corporate research centre of ABB AB in Västerås the same year. He now holds a position as a Senior Principal Scientist focusing on heat and mass transfer for power technologies. He has been working with product development for cables, capacitors, switchgear equipment as well as transformers. He is a member of ASME and IEEE.